

# Journal of Visualized Experiments

## An epithelial abrasion model for studying corneal wound healing

--Manuscript Draft--

<b>Article Type:</b>	Invited Methods Article - JoVE Produced Video
<b>Manuscript Number:</b>	JoVE63112R2
<b>Full Title:</b>	An epithelial abrasion model for studying corneal wound healing
<b>Corresponding Author:</b>	Prince Akowuah University of Houston College of Optometry Houston, Texas UNITED STATES
<b>Corresponding Author's Institution:</b>	University of Houston College of Optometry
<b>Corresponding Author E-Mail:</b>	pkakowua@central.uh.edu
<b>Order of Authors:</b>	Prince Akowuah Angie De La Cruz Wayne Smith Rolando Rumbaut Alan Burns
<b>Additional Information:</b>	
<b>Question</b>	<b>Response</b>
Please specify the section of the submitted manuscript.	Biology
Please indicate whether this article will be Standard Access or Open Access.	Standard Access (\$1400)
Please indicate the <b>city, state/province, and country</b> where this article will be <b>filmed</b> . Please do not use abbreviations.	Houston, Texas, USA
Please confirm that you have read and agree to the terms and conditions of the author license agreement that applies below:	I agree to the <a href="#">Author License Agreement</a>
Please confirm that you have read and agree to the terms and conditions of the video release that applies below:	I agree to the <a href="#">Video Release</a>
Please provide any comments to the journal here.	

**TITLE:**

An Epithelial Abrasion Model for Studying Corneal Wound Healing

**AUTHORS AND AFFILIATIONS:**

Prince K. Akowuah<sup>1</sup>, Angie De La Cruz<sup>1</sup>, C. Wayne Smith<sup>2</sup>, Rolando E. Rumbaut<sup>2,3</sup>, Alan R. Burns<sup>1,2</sup>

<sup>1</sup>University of Houston, College of Optometry, Houston, TX, USA.

<sup>2</sup>Baylor College of Medicine, Children's Nutrition Research Center, Houston, TX, USA.

<sup>3</sup>Center for Translational Research on Inflammatory Diseases (CTRID), Michael E. DeBakey Veterans Affairs Medical Center, Houston, TX, USA.

Email addresses of Co-authors:

Prince K. Akowuah ([pkakowua@central.uh.edu](mailto:pkakowua@central.uh.edu))

Angie De La Cruz ([asdelacr@central.uh.edu](mailto:asdelacr@central.uh.edu))

C. Wayne Smith ([wsmith5413@gmail.com](mailto:wsmith5413@gmail.com))

Rolando E. Rumbaut ([rrumbaut@bcm.edu](mailto:rrumbaut@bcm.edu))

Alan R. Burns ([arburns2@central.uh.edu](mailto:arburns2@central.uh.edu))

Corresponding author:

Prince K. Akowuah ([pkakowua@central.uh.edu](mailto:pkakowua@central.uh.edu))

**KEYWORDS:**

cornea, wound healing, abrasion, golf-club spud, trephine

**SUMMARY:**

Here, a protocol for creating a central corneal epithelial abrasion wound in the mouse using a trephine and a blunt golf club spud is described. This corneal wound healing model is highly reproducible and is now being used to evaluate compromised corneal wound healing in the context of diseases.

**ABSTRACT:**

The cornea is critical for vision, accounting for about two-thirds of the refractive power of the eye. Crucial to the role of the cornea in vision is its transparency. However, due to its external position, the cornea is highly susceptible to a wide variety of injuries that can lead to the loss of corneal transparency and eventual blindness. Efficient corneal wound healing in response to these injuries is pivotal for maintaining corneal homeostasis and preservation of corneal transparency and refractive capabilities. In events of compromised corneal wound healing, the cornea becomes vulnerable to infections, ulcerations, and scarring. Given the fundamental importance of corneal wound healing to the preservation of corneal transparency and vision, a better understanding of the normal corneal wound healing process is a prerequisite to understanding impaired corneal wound healing associated with infection and disease. Toward this goal, murine models of corneal wounding have proven useful in furthering our understanding of the corneal wound healing mechanisms operating under normal physiological conditions. Here, a protocol for creating a central corneal epithelial abrasion in mouse using a trephine and

a blunt golf club spud is described. In this model, a 2 mm diameter circular trephine, centered over the cornea, is used to demarcate the wound area. The golf club spud is used with care to debride the epithelium and create a circular wound without damaging the corneal epithelial basement membrane. The resulting inflammatory response proceeds as a well-characterized cascade of cellular and molecular events that are critical for efficient wound healing. This simple corneal wound healing model is highly reproducible and well-published and is now being used to evaluate compromised corneal wound healing in the context of disease.

## **INTRODUCTION:**

The cornea is the transparent anterior one-third of the eye. The cornea serves several functions including protecting the inner structures of the eye and forming a structural barrier that protects the eye against infections<sup>1</sup>. More importantly, the cornea is critical for vision, providing about two-thirds of the refractive power of the eye<sup>2,3</sup>. Crucial to the role of the cornea in vision is its transparency. However, due to its outward position, the cornea is exposed to a wide variety of injuries on a day-to-day basis that can lead to disruption of its barrier function, loss of transparency, and eventual blindness. Loss of corneal transparency is a leading cause of visual impairment worldwide<sup>4,5</sup>. Corneal abrasions are a common reason for visits to the emergency room (ER), accounting for half of the eye-related cases presented at the ER<sup>6</sup>. Over 1 million individuals are estimated to suffer from eye-related injuries annually in the United States<sup>7</sup>. Efficient corneal wound healing in response to these injuries is pivotal for maintaining corneal homeostasis and preservation of its transparency and refractive capabilities. In events of compromised corneal wound healing, the cornea becomes vulnerable to infections, ulcerations, and scarring<sup>8,9</sup>. Also, the increasing popularity of refractive surgeries places a unique traumatic challenge on the cornea<sup>10</sup>. Given the fundamental importance of corneal wound healing to the preservation of corneal transparency and vision, a better understanding of the normal corneal wound healing process is a prerequisite to understanding impaired corneal wound healing associated with infection and disease.

To that end, several animal models of corneal wound healing have been developed<sup>11-15</sup>. Murine models of corneal wound healing have proven useful in furthering our understanding of the corneal wound healing mechanisms operating under normal physiological conditions. Different types of corneal wounds have been employed in studying corneal wound healing, each suitable for investigating different aspects of the wound healing process. The commonest types of wound models used in corneal wound healing studies are the mechanical and chemical wound models. Chemical corneal wounds, mostly involving the creation of alkaline burns on the cornea, are useful for studying corneal ulcers, opacification, and neovascularization<sup>13</sup>. Mechanical corneal wounds involve debridement (abrasion) wounds and keratectomy wounds<sup>14-16</sup>. An intact or breached corneal epithelial basement membrane defines debridement and keratectomy wounds, respectively. In debridement wounds, the epithelial basement membrane remains intact, while in keratectomy wounds, the basement membrane is breached and is mostly restricted to the anterior stroma. Debridement wounds are most useful for studying re-epithelialization, epithelial cell proliferation, immune response, and nerve regeneration following corneal wounding. Keratectomy wounds, on the other hand, are most useful for studying corneal scarring<sup>14,15</sup>.

Here, a protocol for creating a central corneal epithelial abrasion wound in the mouse using a trephine and a blunt golf club spud is described. This simple corneal wound healing model is highly reproducible and well-published and is now being used to evaluate compromised corneal wound healing in the context of disease<sup>17</sup>.

## **PROTOCOL:**

All animal protocols were approved by the Institutional Animal Care and Use Committees at the University of Houston and Baylor College of Medicine. The guidelines outlined in the Association for Research in Vision and Ophthalmology (ARVO) statement on the use of animals in vision and ophthalmic research were followed in handling and using the mice.

## **1. Preparation**

### **1.1. Preparation of fluorescein solution**

1.1.1. Prepare 1% fluorescein solution by dissolving 10 mg of sodium fluorescein salt in 1 mL of sterile saline or sterile 1x phosphate buffered saline (PBS).

NOTE: Prepare sodium fluorescein solution on the day of use or a day before to avoid microbial contamination. When prepared a day before use, store fluorescein solution at 4 °C away from light. Wrap tubes with aluminum foil to prevent photobleaching.

1.1.2. Divide the solution into aliquots suitable for use in a single experiment. 1–1.5 µL of fluorescein solution is used per mouse per time point. Use the following formula to calculate the volume of aliquot appropriate for a single experiment:

$$(1.5 \times \text{number of mice} \times \text{number of time points}) = \text{Volume of the aliquot}$$

NOTE: For example, if six mice are studied in a single experiment with wound size monitored at five time points, the volume of aliquot suitable for that single experiment would be:

$$1.5 \times 6 \times 5 = 45 \mu\text{L}$$

### **1.2. Preparation of ketamine/xylazine cocktail for anesthesia of mice.**

1.2.1. To prepare 10 mL of cocktail, mix 2.0 mL of ketamine (100 mg/mL) with 1.0 mL of xylazine (20 mg/mL), and add 7.0 mL of sterile PBS. Prepare ketamine/xylazine cocktail a day before or on the day of the surgery.

NOTE: All solutions should be used at room temperature unless stated otherwise.

## **2. Anesthesia**

2.1. Weigh the mouse (8–12 weeks old C57BL/6 wildtype mice) to determine the appropriate amount of anesthetic to administer. Use the two-handed mouse restraint technique to restrain and handle mice for the injection of the anesthetic<sup>18</sup>. Administer ketamine/xylazine cocktail intraperitoneally (i.p.) at a final concentration of 80 mg/kg of ketamine and 8 mg/kg of xylazine.

2.2. Wait until complete anesthesia is achieved before performing corneal wounding on the mouse. Evaluate the depth of anesthesia by assessing the pedal reflex after toe pinch. When adequate anesthesia is achieved, the mouse should not move upon toe pinch.

NOTE: Because mice quickly lose body heat during anesthesia, it is important to provide a source of warmth for mice to prevent hypothermia. Place mice on a heat source (heating pad) during anesthesia and recovery stages.

### 3. Creation of corneal wound

3.1. Wound the right or left eye only. Maintain consistency with the eye (i.e., left or right) that is wounded when moving from mouse to mouse.

NOTE: Because abrasions damage corneal nerves and reduce acuity, wounding both eyes can cause significant discomfort and impairment. Since analgesics have the potential to suppress inflammatory responses, their use may be a confounder in certain experiments aimed at understanding corneal inflammation. Avoiding analgesics in corneal wound experiments was approved by our Institutional Animal Care and Use Committee (IACUC).

#### 3.2. To create the epithelial corneal wound

3.2.1. Under a dissecting microscope, use the 2 mm diameter trephine (see **Figure 1**) to demarcate the center of the cornea, keeping the eye wide open using the thumb and index finger to hold the eyelids. Gently twirl the trephine to make an impression on the corneal epithelium.

NOTE: Care must be taken to not apply excessive pressure when using the trephine as this can result in corneal perforation. Also, care must be taken to position the trephine centrally. The pupils can be used as a landmark to locate the center of the cornea.

3.2.2. Under a dissecting microscope, hold the blunt golf club spud (see **Figure 1**) at approximately 45° from the surface of the cornea within the area demarcated with the trephine. Carefully and continuously scrape the epithelium within the demarcated area with the spud to debride the epithelium.

NOTE: Do not apply excessive force in debridement as that can also cause corneal perforation. The eyes of mice can dry up during the wounding process, making debridement difficult. In such a case, apply sterile PBS to the ocular surface to maintain optimal hydration.

#### 4. Monitoring of wound closure and re-epithelialization

4.1. Pipette 1–1.5  $\mu$ L of 1% fluorescein solution onto the wounded surface and image cornea using a digital microscope with a blue light source.

4.2. Take images within the first minute of fluorescein solution addition to avoid spreading to surrounding epithelium leading to overestimation of wound size. Wounded corneas are imaged at specific times (i.e., 0 h, 12 h, 18 h, 24 h, and 30 h) after wounding.

NOTE: At all time points, imaging is performed under anesthesia; ketamine/xylazine is used at the time of wounding while isoflurane is used at subsequent timepoints. Mice are housed individually in separate cages for the duration of wound closure monitoring. When housed together, mice tend to lick littermate's eyes, a behavior which has been shown to affect wound healing in different tissues<sup>19,20</sup>.

4.3. Analyze captured images and trace wound area, using an image analysis software. The wound area for each time point is expressed as a percentage of the original wound area at 0 h.

#### 5. Immunofluorescence imaging and analysis

5.1. Euthanize mice by an IACUC-approved method (in this case, carbon dioxide overdose followed by cervical dislocation) at desired time points after wounding.

5.2. Harvest eyeballs by gently pressing on the lateral canthus to displace the eyeball using an iris curved scissor. Guide the scissors behind the eyeball to firmly grasp the optic nerve, and then cut the nerve, which allows the eyeball to be removed.

5.3. Fix each eyeball in 1 mL of 1x PBS containing 2% paraformaldehyde for 1 h at room temperature, and then wash three times in 1 mL of 1x PBS for 5 min each.

5.4. Under a dissecting microscope, use a surgical blade to make an incision in the sclera, about 500  $\mu$ m distal to the limbus, and then cut through the globe. Using forceps, gently remove the iris matter from the cornea, and then carefully trim the sclera tissue away, making sure to leave the limbus intact.

5.5. Make four partial radial cuts, each approximately 1 mm in length, which extend from the peripheral cornea and stop short of the center to allow the cornea to flatten.

5.6. Permeabilize and block corneas in 1 mL of 2% bovine serum albumin (BSA) and 0.01% TritonX -100 in 1x PBS for 15 min followed by blocking in 2% BSA in 1x PBS for an additional 45 min at room temperature.

5.7. Incubate corneas overnight at 4 °C in a cocktail of directly labeled unique fluorochrome conjugated antibodies prepared in 1x PBS containing 2% BSA.

NOTE: Antibodies are targeted to label specific cells and tissues of interest. For example, endothelium, neutrophils, and platelets are labeled with anti-CD31<sup>21,22</sup>, anti-Ly-6G<sup>23,24</sup>, and anti-CD41<sup>25,26</sup> antibodies, respectively. 4',6-diamidino-2-phenylindole (DAPI) is added to the antibody cocktail to visualize nuclei.

5.8. After incubation, wash corneas three times in 1x PBS for 15 min each.

5.9. Mount corneas on a microscope slide in a drop of anti-fade fluorescence mounting medium, cover with a coverslip, and image with the desired magnification (4x to 100x objective) using a fluorescence light microscope. Take full-thickness images of the cornea across different regions as illustrated in **Figure 2A**.

NOTE: The pattern of microscopic analysis illustrated in **Figure 2A** is used for analyzing specific regional changes in inflammation and cell division. Both DAPI and Ly-6G staining are used to identify the extravascular neutrophils. With DAPI staining, spherical neutrophils have a distinct horseshoe or donut shaped nucleus (**Figure 2B**).

[Place **Figure 2** here]

## REPRESENTATIVE RESULTS:

**Figure 3** shows a transmission electron micrograph of a corneal wound created with the blunt golf club spud, demonstrating that the epithelium basement membrane is indeed intact after injury.

[Place **Figure 3** here]

This protocol for corneal wounding has been used to extensively characterize the wound healing dynamics for a 2 mm epithelial abrasion wound<sup>27–33</sup>. The ability to monitor the rate of wound closure and re-epithelialization *in vivo* is a central part of this model. As shown in **Figure 4A**, the use of fluorescein solution and a digital microscope with a blue light source enables visualization of the wound size. In this model, wound closure monitoring is performed at the time of wounding (0 h), 12 h, 18 h, 24 h, and 30 h after wounding. **Figure 4B** shows the kinetics of wound closure over 30 h. In 8–12-week-old C57BL/6 wild-type mice, wound closure and re-epithelialization are typically complete 24 h after wounding as illustrated in **Figure 4B** and a well-regulated inflammatory response is fundamental to efficient wound healing<sup>34–36</sup>.

[Place **Figure 4** here]

The inflammatory response to wounding in this model is well characterized. The epithelial abrasion wound elicits a rapid inflammatory response in the corneal limbal vasculature mainly characterized by vasodilation, platelet extravasation in the stroma, and localization to the corneal

limbus<sup>37–39</sup>, neutrophil extravasation in the stroma, and subsequent migration to the center of the cornea<sup>40</sup>. **Figure 5** shows the limbal vasculature of an unwounded cornea with extravascular neutrophils (**Figure 5A**) and a wounded cornea with extravascular platelets and neutrophils (**Figure 5B**).

(Place **Figure 5** here)

In this model, neutrophil infiltration into the cornea is assessed across five distinct regions as illustrated in **Figure 2A**. To determine these distinct regions, an image of the full cornea wholemount is captured, visualizing the limbal vasculature with anti-CD31 staining. The innermost edge of the limbal region on each petal is marked using the limbal vasculature as a guide. The distance from the innermost edge of the limbal region from one petal to the other in the horizontal (x) or vertical (y) direction is measured for each cornea wholemount. For 8–12-week-old C57BL/6 wild-type mice, this distance is ~3.7 mm. This distance covers the peripheral-to-peripheral regions. The center of the cornea wholemount is then calculated as the point corresponding to half of the horizontal or vertical diameter of the wholemount. The paracentral region is 500  $\mu$ m left, right, up, or down from the calculated center. The other fields are all 500  $\mu$ m from the preceding field. Both DAPI and Ly-6G staining are used to identify the extravascular neutrophils. Neutrophil counts in each corneal region from the four quadrants are averaged and expressed as neutrophils per field.

Platelet assessment in this model is performed at the limbus only; during corneal wound healing, platelets extravasate and localize to the limbus<sup>27,37</sup>. The total number of platelets at the limbus are counted, and counts are expressed as platelets/ $\text{mm}^2$  of limbal area. The counts from the four petals can be totaled or averaged.

#### **FIGURE AND TABLE LEGENDS:**

**Figure 1: 2 mm trephine and blunt golf club spud.** The trephine is used to demarcate a circular region at the cornea center, and the golf club spud is used to remove the epithelium within the demarcated region.

**Figure 2: Corneal imaging strategy and neutrophil infiltration after central abrasion. (A)** Schematic representation of a cornea wholemount showing nine microscopic fields across the diameter of the cornea. The gray area represents the original wound area. The width of each region is 500  $\mu$ m. **(B)** Note the distinct horseshoe or donut shape of neutrophil nuclei with DAPI staining.

**Figure 3: Epithelial basement membrane remains intact after corneal abrasion.** Transmission electron micrograph of a corneal wound created with the blunt golf club spud. The arrowheads point to the basement membrane beneath the epithelium surrounding the wound, while the arrows point to the basement membrane in the denuded area. This shows the continuity of the basement membrane from the unabraded to the abraded portions of the cornea, demonstrating that the basement membrane is left intact after debridement.



**Figure 4: Epithelial wound closure was evaluated using fluorescein staining. (A)** Representative images of fluorescein staining of the corneal wound at 0 h, 12 h, 18 h, 24 h, and 30 h. In this model, wound closure and re-epithelialization are typically complete 24 h after wounding. Note the lack of green staining in the central cornea at 24 h and 30 h. **(B)** Wound closure kinetics indicating complete wound closure by 24 h after wounding. Value at each time point is expressed as a percentage of the original wound area (i.e., wound area at 0 h) ( $n \geq 6$ ). Data presented as mean  $\pm$  standard deviation.

**Figure 5: Inflammatory cell imaging at the limbus.** Photomicrograph of the corneal limbus showing staining for the limbal blood vessels with anti-CD31 antibody (shown in red), neutrophils with anti-Ly-6G antibody (shown in green), and platelets with anti-CD41 antibody (shown in blue). **(A)** no abrasion and **(B)** 30 h after abrasion.

## DISCUSSION:

The purpose of this methods paper was to describe a protocol for creating a central corneal epithelial abrasion wound in the mouse using a trephine and a blunt golf club spud. This murine model has been used to study corneal inflammation and its contribution to wound healing. This type of model can be used to study corneal wound healing mechanisms under normal physiological conditions and in pathologies<sup>17,28,29,41,42</sup>. The model has been used to investigate corneal wound healing under pathological conditions as evidenced by a study on impaired corneal wound healing in a mouse model of diet-induced obesity<sup>17</sup>. A distinct advantage of this model is that it creates an exact (2 mm) reproducible epithelial wound size with a precise central location without breaching the basement membrane. This model of corneal wounding is straightforward and quick to perform. In addition to the blunt golf club spud<sup>29,39,43–45</sup>, the rotating burr (Algerbrush)<sup>38,46,47</sup>, and diamond blade<sup>32,37,40,48–51</sup> can both be used to create the abrasion wound in this model. In the hands of an experienced user, there is no substantial difference in the abrasion wound created by either tool. For training purposes and in the hands of a novice, it is often easier to achieve reproducible results with the blunt golf club spud compared to the rotating burr and diamond blade. The rotating burr (Algerbrush) requires a delicate touch otherwise the rotating burr can damage the epithelial basement membrane. This has also been reported by other investigators<sup>52,53</sup>. On the other hand, the blunt golf club spud consistently leaves the epithelial basement membrane intact.

To successfully reproduce this corneal wounding protocol and observe the subsequent re-epithelialization and inflammation dynamics, the same strain and age range of mouse must be used, and the size and the depth of the wound must be created as described above. The corneal wound healing dynamics and timelines described in this protocol are for the C57BL/6 mouse strain and might not be shared if a different strain of mouse is used. Pal-Ghosh et al.<sup>54</sup> reported variations in the ability of C57BL/6 and BALB/c to heal corneal epithelial debridement wounds. For the same corneal wound size, corneal wound closure and re-epithelialization are slower in BALB/c mice. The timeline for completion of wound closure and the characteristic inflammatory response described here are for a 2 mm diameter size circular wound. A longer wound closure

completion time is expected for wound diameters greater than 2 mm while a shorter time is expected for wound diameters less than 2 mm. Also, larger corneal wounds, especially those closer to the limbus, are expected to elicit a more exaggerated inflammatory response, as more leukocytes are recruited into the cornea<sup>16</sup>. More importantly, the wound should be restricted to the corneal epithelium. Wounds breaching the epithelial basement membrane or penetrating the corneal stroma take a longer time to heal. These wounds are also associated with an altered inflammatory response, neovascularization, myofibroblast formation, and scarring<sup>55,56</sup>.

Care must be taken in every step to prevent microbial infection of the abraded cornea. Microbial infection alters the inflammatory response and can lead to ulcerations, scarring, and vision loss<sup>57</sup>. To prevent microbial infection of the wound, sterile tools and solutions should always be used. If multiple mice are being wounded at a time, a sterile trephine should be used for each mouse. In between mice, the golf club spud should be washed in sterile PBS followed by disinfection in 70% ethanol and washed again in sterile PBS. If wounding is performed on additional mice over multiple days, it should be performed at the same time of the day. This is to control the circadian effect on wound healing and inflammation. In C57BL/6 mice, the time of day when the wound is made affects the rate and quality of corneal wound healing. Faster wound closure and greater cell division are observed when mice are wounded in the morning compared to wounding in the afternoon or evening<sup>42</sup>. The circadian effect on wound healing has been reported in other tissues including the skin<sup>58,59</sup>. Wounding in this model is always performed in the morning.

The resulting inflammatory response to wounding in this model proceeds as a well-characterized cascade of cellular and molecular events that are critical for efficient wound healing. The best characterized cellular players in the abrasion-induced inflammation in this model are neutrophils and platelets. Neutrophils are the first responders to the site of corneal abrasion; significant levels of neutrophils are detected in the corneal stroma within 6 h of wounding. Neutrophils are responsible for clearing cell debris, a process intrinsic to inflammation and wound repair<sup>60</sup>. In addition to their phagocytic activities, neutrophils contain growth factors such as vascular endothelial growth factors (VEGF)<sup>61</sup>. VEGF is a crucial neuro-regenerative factor for corneal nerves regeneration following wounding<sup>62,63</sup> and is also important for corneal epithelial cell division<sup>45,63</sup>. Neutrophil infiltration at the limbus occurs in two waves with the first peak at 18 h and the second peak at 30 h after wounding<sup>40</sup>. Using neutropenic mice<sup>37,40</sup>, neutrophil extravasation and subsequent migration to the center of the cornea have been shown to be crucial for corneal wound healing. Although traditionally known to be pivotal in the maintenance of hemostasis and blood clotting, platelets also have a recognized key role in corneal wound healing<sup>37</sup>. Platelets contain numerous mediators that contribute to inflammation and tissue resolution<sup>64,65</sup>. In mice with thrombocytopenia, this model has been used to show that platelets are important for efficient corneal wound healing<sup>37</sup>.

Although neutrophils and platelets are the best-characterized cells in this model, immune cells such as gamma delta T-cells, natural killer cells, and dendritic cells have also been shown to be involved in the immune response to wounding using this model<sup>27,48</sup>. Natural killer cell extravasation in the stroma<sup>28,29</sup> and migration of gamma delta T cells into the healing epithelium<sup>27</sup> have been reported. This model has also been used to identify adhesion molecules

key to immune cell extravasation during corneal wound healing. Lymphocyte function antigen-1 (LFA-1)<sup>32</sup>, CD18<sup>51</sup>, and intercellular adhesion molecule-1 (ICAM-1)<sup>47,49</sup> have all been shown to be crucial for neutrophil extravasation and efficient corneal wound healing using this model. Epithelial cell division in response to wounding, which is critical for epithelial re-stratification after wound closure is assessed using mitotic figures. Chromosomal condensation during different stages of cell division gives the nuclei a characteristic appearance known as a mitotic figure. DAPI staining of the nucleus enables visualization of these mitotic figures.

The mouse corneal abrasion wound model has proven to be remarkably reproducible and provided considerable insight into the cellular and molecular mechanisms that contribute to efficient wound healing. However, it is worth noting that there are limitations to the model with regard to its clinical applicability. The model and its outcomes are only applicable to simple, non-penetrating epithelial abrasions. As noted earlier, corneal injuries resulting from penetrating wounds caused by physical or chemical insult will elicit different wound healing kinetics and outcomes, particularly if the wound becomes infected as occurs often in the case of injuries to the human cornea. That being said, the mouse corneal abrasion wound model does provide an excellent foundation for studying fundamental principles of inflammation that modulate corneal wound healing.

The corneal wounding protocol described here is straightforward and easily reproduced. It provides a useful tool to investigate fundamental questions about the corneal wound healing process and its associated inflammatory response. Its potential to aid in understanding corneal pathologies associated with wound healing complications is just the beginning.

#### **ACKNOWLEDGMENTS:**

Funding: Supported by: NIH EY018239 (A.R.B., C.W.S., and R.E.R.), P30EY007551 (A.R.B.), and Sigma Xi Grant in Aid of Research (P.K.A.). The content is solely the responsibility of the authors and does not represent the official views of the National Institutes of Health, or Sigma Xi.

#### **DISCLOSURES:**

The authors have nothing to disclose.

#### **REFERENCES:**

1. DelMonte, D. W., Kim, T. Anatomy and physiology of the cornea. *Journal of Cataract and Refractive Surgery*. **37** (3), 588–598 (2011).
2. Meek, K. M., Knupp, C. Corneal structure and transparency. *Progress in Retinal and Eye Research*. **49**, 1–16 (2015).
3. Sridhar, M. S. Anatomy of cornea and ocular surface. *Indian Journal of Ophthalmology*. **66** (2), 190–194 (2018).
4. Flaxman, S. R. et al. Global causes of blindness and distance vision impairment 1990–2020: a systematic review and meta-analysis. *The Lancet Global Health*. **5** (12), e1221–e1234 (2017).
5. Robaei, D., Watson, S. Corneal blindness: A global problem. *Clinical & Experimental*

- 440 *Ophthalmology*. **42** (3), 213–214 (2014).
- 441 6. McGwin, G., Owsley, C. Incidence of emergency department-treated eye injury in the  
442 United States. *Archives of Ophthalmology*. **123** (5), 662–666 (2005).
- 443 7. Ljubimov, A. V., Saghizadeh, M. Progress in corneal wound healing. *Progress in Retinal*  
444 *and Eye Research*. **49**, 17–45 (2015).
- 445 8. Wilson, S. L., Haj, A. J. E., Yang, Y. Control of scar tissue formation in the cornea: Strategies  
446 in clinical and corneal tissue engineering. *Journal of Functional Biomaterials*. **3** (3), 642 (2012).
- 447 9. Vaidyanathan, U. et al. Persistent corneal epithelial defects: A review article. *Medical*  
448 *Hypothesis, Discovery and Innovation in Ophthalmology*. **8** (3), 163–176 (2019).
- 449 10. Netto, M. et al. Wound healing in the cornea: a review of refractive surgery complications  
450 and new prospects for therapy. *Cornea*. **24** (5), 509–522 (2005).
- 451 11. Friedenwald, J. S., Buschke, W. Some factors concerned in the mitotic and wound-healing  
452 activities of the corneal epithelium. *Transactions of the American Ophthalmological Society*. **42**,  
453 371–383 (1944).
- 454 12. Xu, K., Yu, F.-S. X. Impaired epithelial wound healing and EGFR signaling pathways in the  
455 corneas of diabetic rats. *Investigative Ophthalmology & Visual Science*. **52** (6), 3301–3308 (2011).
- 456 13. Bai, J. Q., Qin, H. F., Zhao, S. H. Research on mouse model of grade II corneal alkali burn.  
457 *International Journal of Ophthalmology*. **9** (4), 487–490 (2016).
- 458 14. Blanco-Mezquita, J. T., Hutcheon, A. E. K., Stepp, M. A., Zieske, J. D.  $\alpha$ V $\beta$ 6 integrin  
459 promotes corneal wound healing. *Investigative Ophthalmology and Visual Science*. **52** (11), 8505–  
460 8513 (2011).
- 461 15. Blanco-Mezquita, J. T., Hutcheon, A. E. K., Zieske, J. D. Role of thrombospondin-1 in repair  
462 of penetrating corneal wounds. *Investigative Ophthalmology and Visual Science*. **54** (9), 6262–  
463 6268 (2013).
- 464 16. Stepp, M. A. et al. Wounding the cornea to learn how it heals. *Experimental Eye Research*.  
465 **121**, 178–193 (2014).
- 466 17. Hargrave, A. et al. Corneal dysfunction precedes the onset of hyperglycemia in a mouse  
467 model of diet-induced obesity. *PLoS ONE*. **15**, e0238750 (2020).
- 468 18. Machholz, E., Mulder, G., Ruiz, C., Corning, B. F., Pritchett-Corning, K. R. Manual restraint  
469 and common compound administration routes in mice and rats. *Journal of Visualized*  
470 *Experiments: JoVE*. (67), 2771 (2012).
- 471 19. Bodner, L., Dayan D. Effect of parotid submandibular and sublingual saliva on wound  
472 healing in rats. *Comparative Biochemistry and Physiology. Part A, Physiology*. **100** (4), 887–890  
473 (1991).
- 474 20. Abbasian, B., Azizi, S., Esmaeili, A. Effects of rat's licking behavior on cutaneous wound  
475 healing. *Iranian Journal of Basic Medical Sciences*. **13** (1), 242–247 (2010).
- 476 21. DeLisser, H. M. et al. Involvement of endothelial PECAM-1/CD31 in angiogenesis. *The*  
477 *American Journal of Pathology*. **151** (3), 671–677 (1997).
- 478 22. Piali, L. et al. CD31/PECAM-1 is a ligand for alpha v beta 3 integrin involved in adhesion of  
479 leukocytes to endothelium. *The Journal of Cell Biology*. **130** (2), 451–460 (1995).
- 480 23. Fleming, T. J., Fleming, M. L., Malek, T. R. Selective expression of Ly-6G on myeloid lineage  
481 cells in mouse bone marrow. RB6-8C5 mAb to granulocyte-differentiation antigen (Gr-1) detects  
482 members of the Ly-6 family. *The Journal of Immunology*. **151** (5), 2399–2408 (1993).
- 483 24. Fleming, T. J., Malek, T. R. Multiple glycosylphosphatidylinositol-anchored Ly-6 molecules

484 and transmembrane Ly-6E mediate inhibition of IL-2 production. *The Journal of Immunology*. **153**  
485 (5), 1955–1962 (1994).

486 25. Phillips, D. R., Charo, I. F., Scarborough, R. M. GPIIb-IIIa: the responsive integrin. *Cell*. **65**  
487 (3), 359–362 (1991).

488 26. Nieswandt, B. et al. Acute systemic reaction and lung alterations induced by an  
489 antiplatelet integrin gplIb/IIIa antibody in mice. *Blood*. **94** (2), 684–693 (1999).

490 27. Li, Z., Burns, A. R., Rumbaut, R. E., Smith, C. W.  $\gamma\delta$  T cells are necessary for platelet and  
491 neutrophil accumulation in limbal vessels and efficient epithelial repair after corneal abrasion.  
492 *American Journal of Pathology*. **171** (3), 838–845 (2007).

493 28. Liu, Q., Smith, C. W., Zhang, W., Burns, A. R., Li, Z. NK cells modulate the inflammatory  
494 response to corneal epithelial abrasion and thereby support wound healing. *American Journal of*  
495 *Pathology*. **181** (2), 452–462 (2012).

496 29. Gao, Y. et al. NK cells are necessary for recovery of corneal CD11c+ dendritic cells after  
497 epithelial abrasion injury. *Journal of Leukocyte Biology*. **94** (2), 343–351 (2013).

498 30. Xiao, C. et al. Acute tobacco smoke exposure exacerbates the inflammatory response to  
499 corneal wounds in mice via the sympathetic nervous system. *Communications Biology*. **2**, 33  
500 (2019).

501 31. Wang, H. et al. Epothilone B speeds corneal nerve regrowth and functional recovery  
502 through microtubule stabilization and increased nerve beading. *Scientific Reports*. **8** (1), 2647  
503 (2018).

504 32. Li, Z., Burns, A. R., Smith, C. W. Lymphocyte function-associated Antigen-1-dependent  
505 inhibition of corneal wound healing. *Cell Injury*. **169**, 1590–1600 (2006).

506 33. Wu, M. et al. The neuroregenerative effects of topical decorin on the injured mouse  
507 cornea. *Journal of Neuroinflammation* 2020 17:1. **17** (1), 1–14 (2020).

508 34. Rodrigues, M., Kosaric, N., Bonham, C. A., Gurtner, G. C. Wound healing: A cellular  
509 perspective. *Physiological Reviews*. **99** (1), 665–706 (2019).

510 35. Rennard, S. I. Inflammation and repair processes in chronic obstructive pulmonary  
511 disease. *American Journal of Respiratory and Critical Care Medicine*. **160** (5 Pt 2), S12–S16 (1999).

512 36. Landén, N. X., Li, D., Ståhle, M. Transition from inflammation to proliferation: a critical  
513 step during wound healing. *Cellular and Molecular Life Sciences*. **73** (20), 3861–3885 (2016).

514 37. Li, Z., Rumbaut, R. E., Burns, A. R., Smith, C. W. Platelet response to corneal abrasion is  
515 necessary for acute inflammation and efficient re-epithelialteation. *Investigative Ophthalmology*  
516 *and Visual Science*. **47**, 4794–4802 (2006).

517 38. Lam, F. W., Burns, A. R., Smith, C. W., Rumbaut, R. E. Platelets enhance neutrophil  
518 transendothelial migration via P-selectin glycoprotein ligand-1. *American Journal of Physiology -*  
519 *Heart and Circulatory Physiology*. **300** (2), H468–H475 (2011).

520 39. Cruz, A. D. La et al. Platelet and erythrocyte extravasation across inflamed corneal venules  
521 depend on CD18, neutrophils, and mast cell degranulation. *International Journal of Molecular*  
522 *Sciences*. **22** (14), 7360 (2021).

523 40. Li, Z., Burns, A. R., Smith, C. W. Two waves of neutrophil emigration in response to corneal  
524 epithelial abrasion: Distinct adhesion molecule requirements. *Investigative Ophthalmology and*  
525 *Visual Science*. **47** (5), 1947–1955 (2006).

526 41. Li, Z., Burns, A. R., Han, L., Rumbaut, R. E., Smith, C. W. IL-17 and VEGF Are Necessary for  
527 Efficient Corneal Nerve Regeneration. *The American Journal of Pathology*. **178** (3), 1106–1116

(2011).

42. Xue, Y. et al. Modulation of circadian rhythms affects corneal epithelium renewal and repair in mice. *Investigative Ophthalmology and Visual Science*. **58** (3), 1865–1874 (2017).

43. Zhang, W., Magadi, S., Li, Z., Smith, C. W., Burns, A. R. IL-20 promotes epithelial healing of the injured mouse cornea. *Experimental Eye Research*. **154**, 22–29 (2017).

44. Li, Z., Burns, A. R., Miller, S. B., Smith, C. W. CCL20,  $\gamma\delta$  T cells, and IL-22 in corneal epithelial healing. *FASEB Journal*. **25** (8), 2659–2668 (2011).

45. Li, Z., Burns, A. R., Han, L., Rumbaut, R. E., Smith, C. W. IL-17 and VEGF are necessary for efficient corneal nerve regeneration. *American Journal of Pathology*. **178** (3), 1106–1116 (2011).

46. Reins, R. Y., Hanlon, S. D., Magadi, S., McDermott, A. M. Effects of topically applied Vitamin D during corneal wound healing. *PLoS ONE*. **11** (4), e0152889 (2016).

47. Gagen, D. et al. ICAM-1 mediates surface contact between neutrophils and keratocytes following corneal epithelial abrasion in the mouse. *Experimental Eye Research*. **91** (5), 676–684 (2010).

48. Li, Z., Rivera, C. A., Burns, A. R., Smith, C. W. Hindlimb unloading depresses corneal epithelial wound healing in mice. *Journal of Applied Physiology*. **97** (2), 641–647 (2004).

49. Byeseda, S. E. et al. ICAM-1 is necessary for epithelial recruitment of  $\gamma\delta$  T cells and efficient corneal wound healing. *American Journal of Pathology*. **175** (2), 571–579 (2009).

50. Li, Z., Burns, A. R., Rumbaut, R. E., Smith, C. W.  $\gamma\delta$  T cells are necessary for platelet and neutrophil accumulation in limbal vessels and efficient epithelial repair after corneal abrasion. *American Journal of Pathology*. **171** (3), 838–845 (2007).

51. Petrescu, M. S. et al. Neutrophil interactions with keratocytes during corneal epithelial wound healing: A role for CD18 integrins. *Investigative Ophthalmology and Visual Science*. **48** (11), 5023–5029 (2007).

52. Pal-Ghosh, S., Pajoohesh-Ganji, A., Tadvalkar, G., Stepp, M. A. Removal of the basement membrane enhances corneal wound healing. *Experimental Eye Research*. **93** (6), 927–936 (2011).

53. Pal-Ghosh, S. et al. Cytokine deposition alters leukocyte morphology and initial recruitment of monocytes and  $\gamma\delta$  T cells after corneal injury. *Investigative Ophthalmology & Visual Science*. **55** (4), 2757–2765 (2014).

54. Pal-Ghosh, S., Tadvalkar, G., Jurjus, R. A., Zieske, J. D., Stepp, M. A. BALB/c and C57BL6 mouse strains vary in their ability to heal corneal epithelial debridement wounds. *Experimental Eye Research*. **87** (5), 478–486 (2008).

55. Kato, T., Chang, J. H., Azar, D. T. Expression of type XVIII collagen during healing of corneal incisions and keratectomy wounds. *Investigative Ophthalmology and Visual Science*. **44** (1), 78–85 (2003).

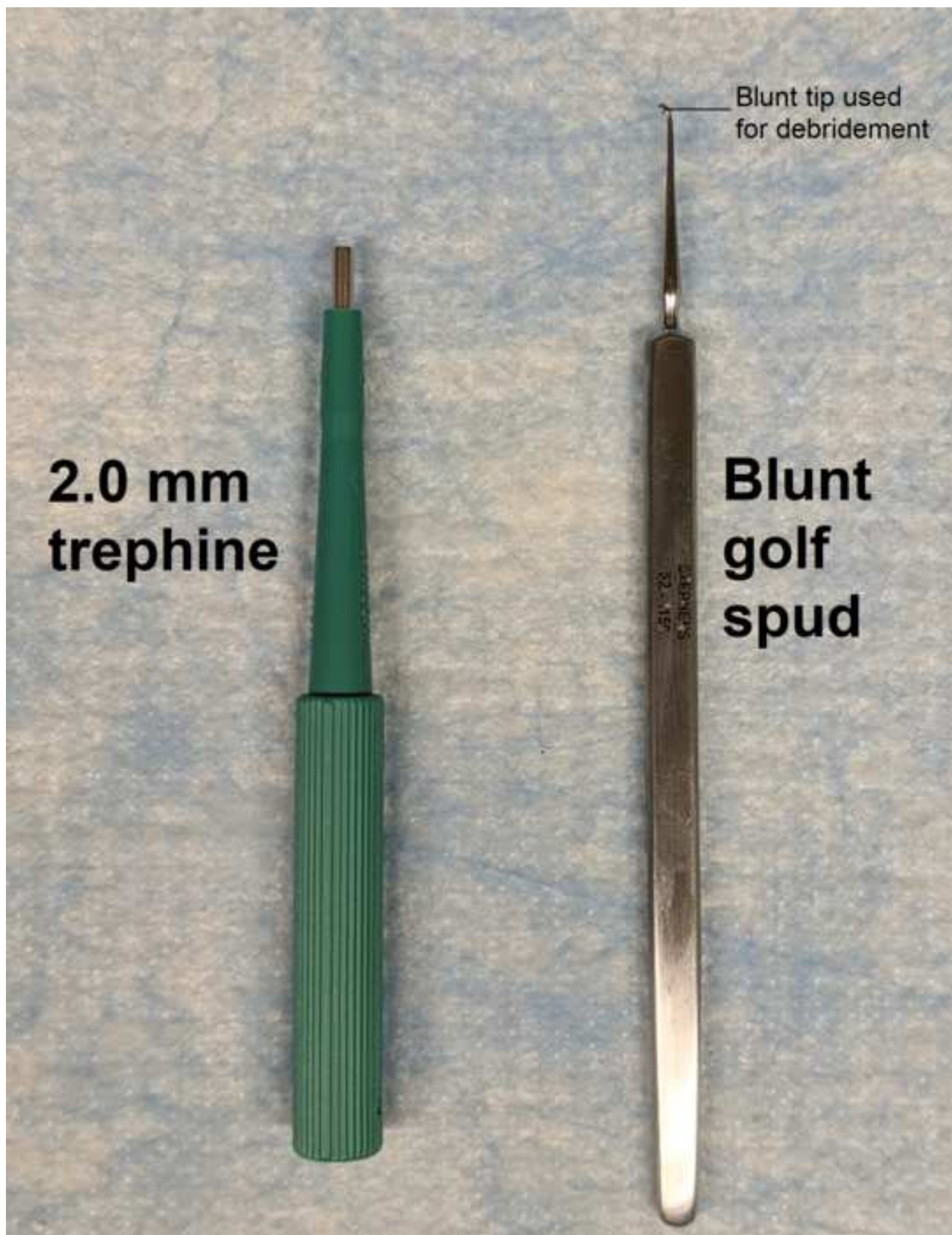
56. Kure, T. et al. Corneal neovascularization after excimer keratectomy wounds in matrilysin-deficient mice. *Investigative Ophthalmology and Visual Science*. **44** (1), 137–144 (2003).

57. Lin, A. et al. Bacterial keratitis preferred practice pattern. *Ophthalmology*. **126** (1), P1–P55 (2019).

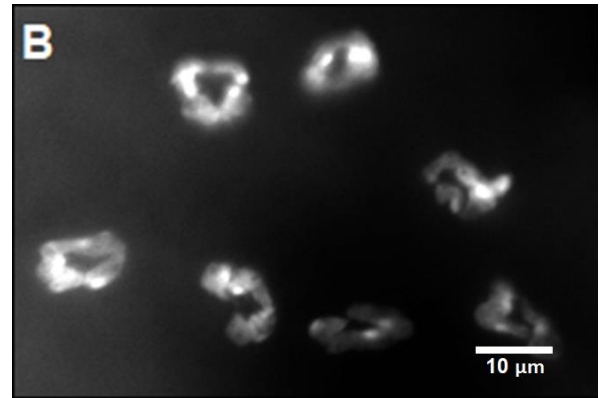
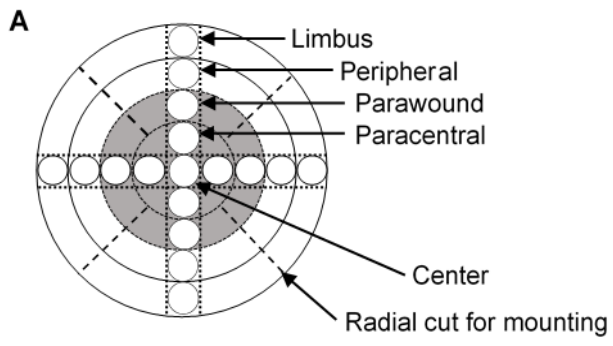
58. Cable, E. J., Onishi, K. G., Prendergast, B. J. Circadian rhythms accelerate wound healing in female Siberian hamsters. *Physiology and Behavior*. **171**, 165–174 (2017).

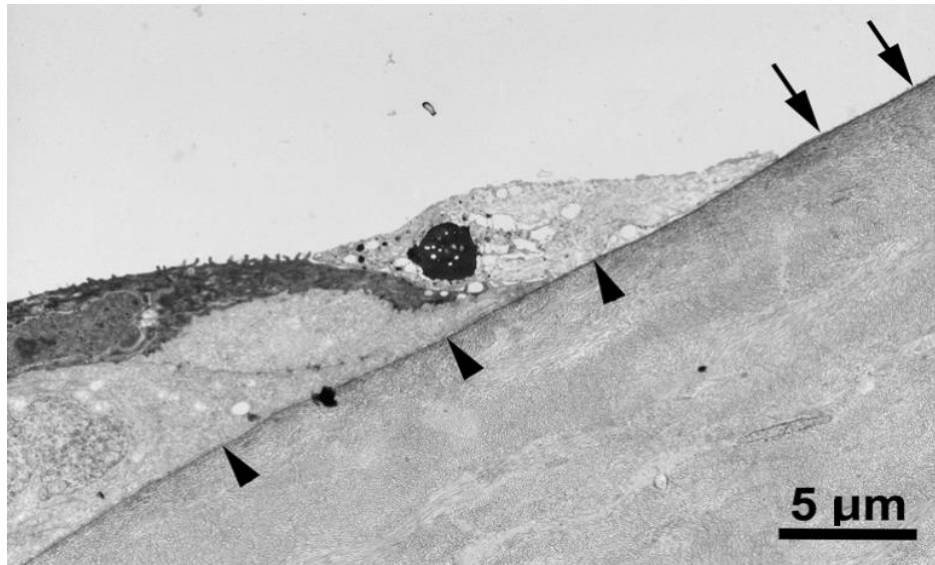
59. Lyons, A. B., Moy, L., Moy, R., Tung, R. Circadian rhythm and the skin: A review of the literature. *Journal of Clinical and Aesthetic Dermatology*. **12** (9), 42–45 at </pmc/articles/PMC6777699/> (2019).

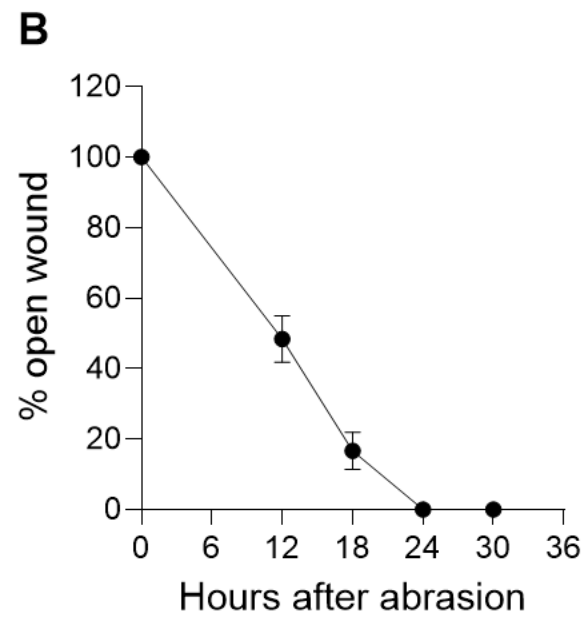
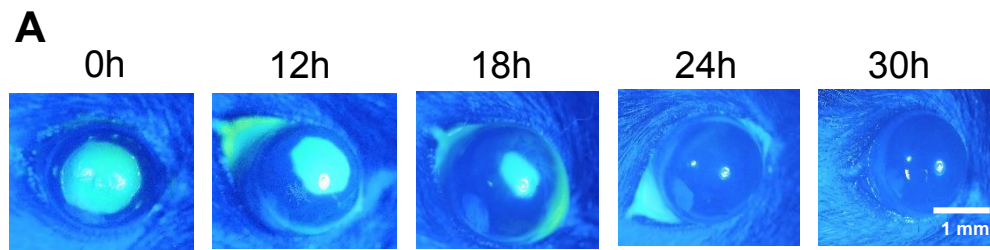
- 572 60. Westman, J., Grinstein, S., Marques, P. E. Phagocytosis of Necrotic Debris at Sites of Injury  
573 and Inflammation. *Frontiers in Immunology*. **10**, 3030 (2020).
- 574 61. Gaudry, M. et al. Intracellular pool of vascular endothelial growth factor in human  
575 neutrophils. *Blood*. **90** (10), 4153–4161 (1997).
- 576 62. Pan, Z. et al. Vascular endothelial growth factor promotes anatomical and functional  
577 recovery of injured peripheral nerves in the avascular cornea. *FASEB Journal*. **7**, 2756–2767  
578 (2013).
- 579 63. Di, G. et al. VEGF-B promotes recovery of corneal innervations and trophic functions in  
580 diabetic mice. *Scientific Reports*. **7** (1), 1–13 (2017).
- 581 64. Thomas, M. R., Storey, R. F. The role of platelets in inflammation. *Thrombosis and*  
582 *Haemostasis*. **114** (3), 449–458 (2015).
- 583 65. Margraf, A., Zarbock, A. Platelets in inflammation and resolution. *The Journal of*  
584 *Immunology*. **203** (9), 2357–2367 (2019).
- 585

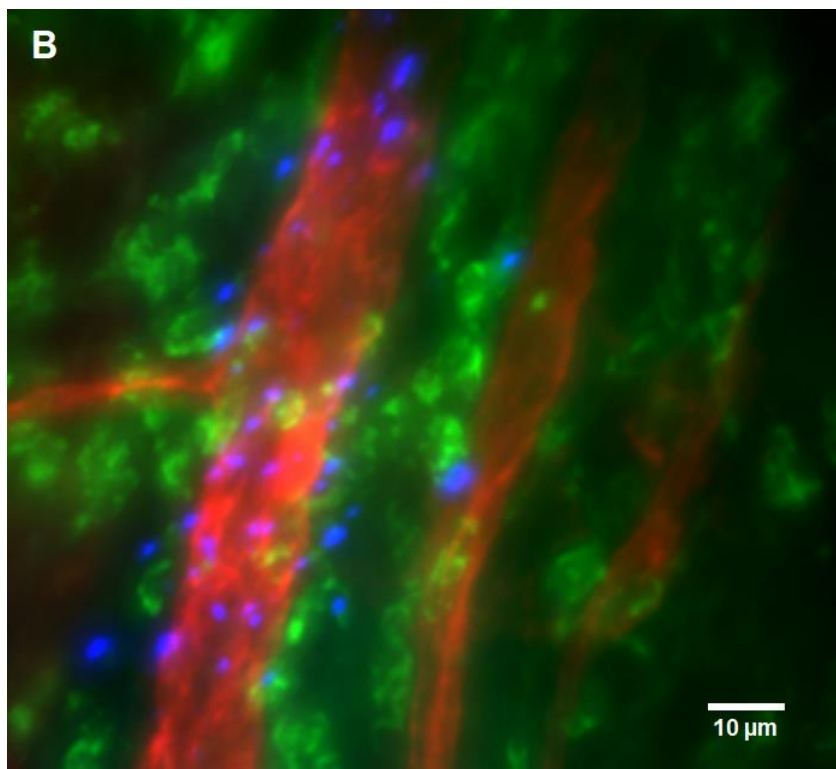
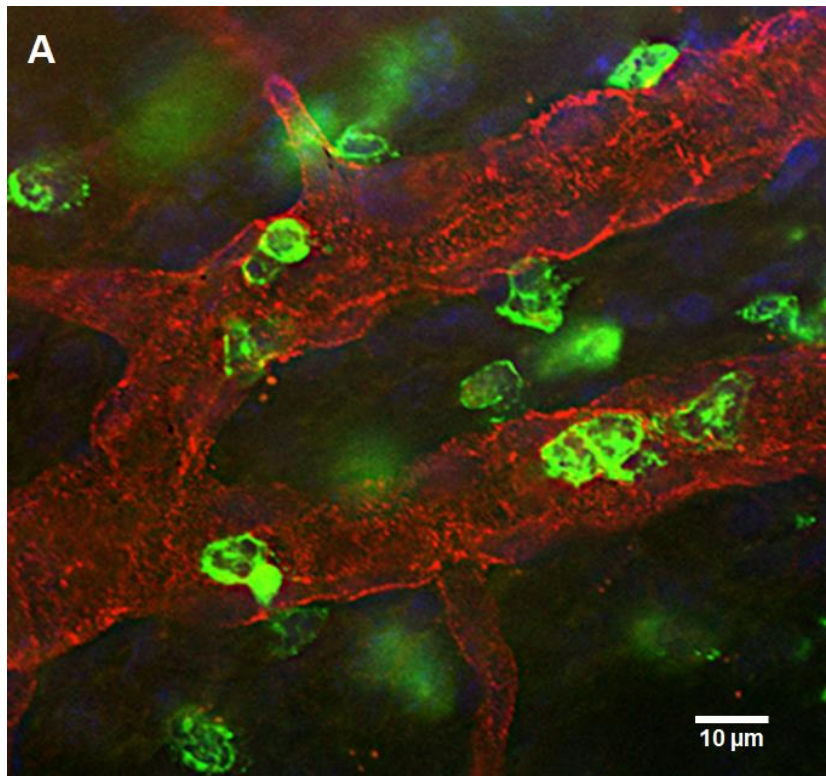














### Editorial comments

The editor has formatted the manuscript to match the journal's style. Please retain and use the attached version for revision.

Authors' response

Alright

2. Please address all the specific comments marked in the manuscript.

Authors' response

Done

3. Please ensure that the highlighting is no more than 3 pages including headings and spacings and is in line with the title of the manuscript.

Authors' response

Alright